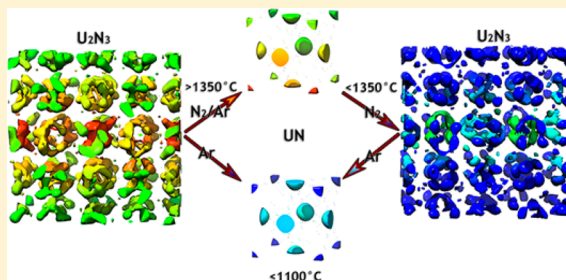


Synthesis of Phase-Pure U_2N_3 Microspheres and Its Decomposition into UN

Chinthaka M. Silva,* Rodney D. Hunt, Lance L. Snead, and Kurt A. Terrani

Materials Science and Technology Division, Oak Ridge National Laboratory, Oak Ridge, Tennessee 37831, United States

ABSTRACT: Uranium mononitride (UN) is important as a nuclear fuel. Fabrication of UN in its microspherical form also has its own merits since the advent of the concept of accident-tolerant fuel, where UN is being considered as a potential fuel in the form of TRISO particles. However, not many processes have been well established to synthesize kernels of UN. Therefore, a process for synthesis of microspherical UN with a minimum amount of carbon is discussed herein. First, a series of single-phased microspheres of uranium sesquinitride (U_2N_3) were synthesized by nitridation of UO_2+C microspheres at a few different temperatures. Resulting microspheres were of low-density U_2N_3 and decomposed into low-density UN. The variation of density of the synthesized sesquinitrides as a function of its chemical composition indicated the presence of extra (interstitial) nitrogen atoms corresponding to its hyperstoichiometry, which is normally indicated as $\alpha\text{-U}_2\text{N}_3$. Average grain sizes of both U_2N_3 and UN varied in a range of 1–2.5 μm . These also had a considerably large amount of pore spacing, indicating the potential sinterability of UN toward its use as a nuclear fuel.



1. INTRODUCTION

Uranium nitrides have been studied quite extensively by both experimental and theoretical means. The main chemical compositions of this system consist of uranium dinitride (UN_2), uranium sesquinitride (U_2N_3), and uranium mononitride (UN), which has been considered as a nonoxide fuel for advanced reactors such as liquid metal-cooled fast reactors (FR) and high-temperature gas-cooled reactors (HTGR). Also, uranium mononitride is being investigated for light water reactors (LWR) in the form of tristructural isotropic (TRISO) particles, as an accident-tolerant fuel. TRISO particle fuel enables superior fission product retention under both normal operating and accident conditions. The fuel UN is important as it has a high fissile density and advantageous neutronic and thermal properties (melting or disintegration point of UN is $3075P_{\text{N}_2}^{0.02832}$ for $P_{\text{N}_2} = 10^{-12}$ – $7.5 \text{ MPa}^{1,2}$) such as high thermal conductivity ($1.864e^{-2.14P}T^{0.361}$ in $\text{W/m}\cdot\text{K}$, where P is the share of porosity) compared to traditional oxide fuels. Because of these favorable properties, especially the high fissile density, of UN compared to UO_2 , use of UN as the core fuel is more practical than use of UO_2 in TRISO particles. Moreover, actinide nitrides (AnN) have unique chemical characteristics such as good solid-phase solubility with each other. This allows production of mixed actinide nitrides such as $(\text{U}, \text{Pu})\text{N}$ as a nuclear fuel and as well as to burn excess plutonium.³

For TRISO particle fuel fabrication the nuclear fuel (UN) needs to be in microspherical form. The most common method we have at the present time in synthesizing microspheres of UN or more precisely $\text{UC}_{1-x}\text{N}_x$ is the carbothermic reduction.⁴ In this method, microspheres of UO_2 mixed with carbon are heat treated to temperatures above 1400°C to obtain high-density intermediate kernels containing a mixture of UO_2 and UC.

These kernels are further heated in N_2 to convert the material into UN. In order to obtain high densities ($\geq 95\%\text{TD}$), UN kernels need to be sintered at high temperatures ($>1700^\circ\text{C}$). The literature discusses many different experimental conditions in achieving high densities, as it is a challenging task; however, the reproducibility of these densities has been a difficulty in most of the cases.

Since UN fabrication is challenging, other efforts identifying possible versatile methods is important. In the present study, we discuss the use of another route in synthesizing UN microparticles via an intermediate uranium sesquinitride (U_2N_3) and the characteristics of these two nitrides synthesized at a few different temperatures. The role of N/U molar ratio in U_2N_3 toward its density variation and formation of U_2N_3 via possible reaction of UN with reaction gas N_2 are also discussed. Further investigation of this method is to be carried out to identify the potential of this pathway for the final goal of synthesizing terminal high-density UN for coating to make TRISO particles.

2. EXPERIMENTAL DETAILS

2.1. Solid-State Synthesis of Uranium Nitrides. The starting material used here was air-dried $\text{UO}_3\cdot x\text{H}_2\text{O}+2.65\text{C}$ kernels, which was synthesized by an internal-gelation process.⁵ The air-dried $\text{UO}_3\cdot x\text{H}_2\text{O}+2.65\text{C}$ kernels were either used directly or after calcining in the synthesis of nitrides. Calcination of the air-dried $\text{UO}_3\cdot x\text{H}_2\text{O}+2.65\text{C}$ kernels involve heating the kernels at 600 – 700°C for 2 h in flowing argon gas at a $3^\circ\text{C}/\text{min}$; this step converts the precursor material into $\text{UO}_2+2.15\text{C}$. The average radius of the calcined particles was $765 \mu\text{m}$.

Received: October 7, 2014

Published: December 12, 2014

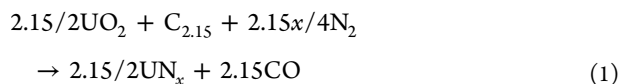


containing a C/U molar ratio of 2.15. Close to 1 g of calcined kernels of UO_2 containing carbon in an Nb-1Zr or Mo crucible was heat treated in flowing nitrogen (N_2) gas, and eight samples were fabricated at eight temperatures from 1100–1800 °C at a 100 °C increment. Flowing $\text{N}_2(\text{g})$ was used as the cover gas all the way until the samples were cooled down to room temperature. Holding times of 10, 20, 30, and 50 h were tested at 1100 °C and 10 h at each other experimenting temperature used. Decomposition of the higher nitride from the second step, U_2N_3 , was performed under flowing argon gas at 1100 °C with a holding time of 2 h at that temperature. Two hours was used to give enough time to complete decomposition of U_2N_3 into UN since 30 min was used in another study reported by Silva et al.⁶ Sintering of the product UN was also carried out in flowing argon, vacuum, N_2 –4% H_2 , and Ar–4% H_2 . Sintering experimental conditions are reported in the text where results are discussed.

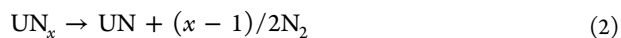
2.2. Characterization Methods. The average particle size was determined using optical microscopic images of randomly selected kernels. The mean average particle weight was also determined using five riffled samples. Geometrical densities of the kernels were calculated using average particle weights and volumes. A Mettler Toledo XP504 Analytical Balance was used to weigh the samples. The balance was validated before and after its use with reference weights of 50, 100, 200, and 500 g with calibrated accuracies of ± 0.000024 , ± 0.000031 , ± 0.000053 , and ± 0.000086 g, respectively. A scanning electron microscope, SEM (JEOL 6500 FEG-SEM system), was utilized to investigate microstructural characteristics of the nitride samples. Crystalline chemical phases were identified using powder X-ray diffractometry (XRD); a Scintag XRD instrument using 40 kV and 40 mA with Cu $K\alpha$ radiation was used. The microsphere particles were powdered and mounted on a zero-background XRD sample mount, which was sealed using a Kapton tape, to acquire XRD powder patterns. An internal standard Si SRM640b was used with the samples for lattice parameter refinements using the GSAS⁷ software.

3. RESULTS

3.1. Synthesis of $\text{U}_2\text{N}_{3\pm x}$ and UN. The reactant $\text{UO}_2+2.15\text{C}$ kernels were not fully nitridized at 1100 °C for holding times up to 30 h; the XRD powder patterns showed the presence of $\text{U}_2\text{N}_{3\pm x}$ and the unreacted UO_2 in the samples. Complete transformation of $\text{UO}_2+2.15\text{C}$ into $\text{U}_2\text{N}_{3\pm x}$ was observed when using a holding time of 50 h at 1100 °C. Nitridation of $\text{UO}_2+2.15\text{C}$ kernels at all other seven tested temperatures (>1100 °C) was complete after 10 h of holding time at each temperature. Since no other chemical phase, except for $\text{U}_2\text{N}_{3\pm x}$ and the unreacted UO_2 , was identified in the partially converted samples, it is hypothesized that the incorporated carbon in the UO_2 kernels facilitated the higher uranium nitride formation according to reaction 1 in N_2 environment at 1 atm pressure.



The presence of graphite was not observed in the powder XRD patterns in any of these samples. The higher nitrides (U_2N_3) can be completely decomposed into the corresponding mononitride (UN) at temperatures ≥ 1100 °C.⁶ Therefore, the $\text{U}_2\text{N}_{3\pm x}$ samples were decomposed by heating them at 1100 °C for up to 2 h in flowing argon gas. The resulting product was identified as the uranium mononitride for each sample by powder XRD. The expected reaction for this step is as follows



3.2. Characterization of $\text{U}_2\text{N}_{3\pm x}$ and UN. The uranium nitride samples synthesized by nitriding $\text{UO}_2+2.15\text{C}$ reactant samples in flowing N_2 atmosphere were first characterized using

powder XRD. The sample prepared at 1100 °C with a holding time of 10 h indicated the presence of UN_x with UO_2 as the primary chemical phase. Preliminary analysis of the XRD pattern indicated the UN_x phase in the sample to be UN_2 (a chemical composition of high end of x in UN_x). The intensities of the four major XRD peaks that correspond to (222), (400), (440), and (622) reflections of the UN_x phase at 2θ angles of 28.9°, 33.7°, 48.4°, and 57.2°, respectively, were significantly low for the 10 h sample. Therefore, the presence of minor XRD peaks corresponding to reflections such as (411) and (431) of U_2N_3 phase were not prominent in this sample. However, these minor peaks at 2θ values of 35.6°, 43.2°, and 52.9° in the XRD pattern that correspond to U_2N_3 phase started to appear in the samples synthesized using longer holding times (30 and 50 h) at the same temperature. Some of these minor peaks are highlighted by vertical boxes in the XRD patterns of the samples in Figure 1. Note that the XRD patterns in Figure 1 are

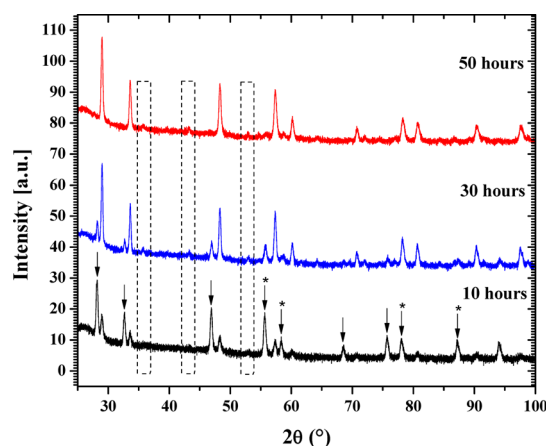


Figure 1. Experimental XRD patterns of the samples heat treated at 1100 °C in flowing N_2 gas as a function of three holding times at that temperature. Arrows indicate peaks corresponding to UO_2 phase. Asterisks are shown on some peaks corresponding to UO_2 that overlap with UN_x peaks. The rest of the peaks correspond to UN_x . Vertical boxes highlight the appearance of minor peaks of the U_2N_3 phase as a function of holding time.

shown starting from a 2θ value of 25° in order to avoid high background at lower angles that corresponds to the Kapton tape used to seal the samples.

After confirming the presence of $\text{U}_2\text{N}_{3\pm x}$ in the samples synthesized at 1100 °C, two more samples at 1200 and 1300 °C were synthesized using the lowest holding time (10 h) tested for the 1100 °C sample. An example of the fitted XRD pattern using Rietveld analysis for the $\text{U}_2\text{N}_{3\pm x}$ synthesized at 1300 °C is shown at the top of Figure 2. As depicted by the U_2N_3 model unit cell shown at the bottom of Figure 2, this unit cell consists of 32 U atoms at 8b and 24d sites in the space group $Ia\bar{3}$. Nitrogen atoms reside on 48e sites of the U_2N_3 unit cell.

Powder XRD of UN prepared by decomposing $\text{U}_2\text{N}_{3\pm x}$ which was made at 1100 °C, contained 19 wt % of the secondary UO_2 phase. Some minor peaks that correspond to (111), (200), and (220) reflections of UO_2 were also observed in the UN samples made by decomposing $\text{U}_2\text{N}_{3\pm x}$ which was made at 1200 °C. When $\text{U}_2\text{N}_{3\pm x}$ made at 1300 °C was used, the UN sample was free of UO_2 according to powder XRD. This indicates that a small amount of UO_2 could be present, mainly in an amorphous state, in the precursor $\text{U}_2\text{N}_{3\pm x}$ samples made

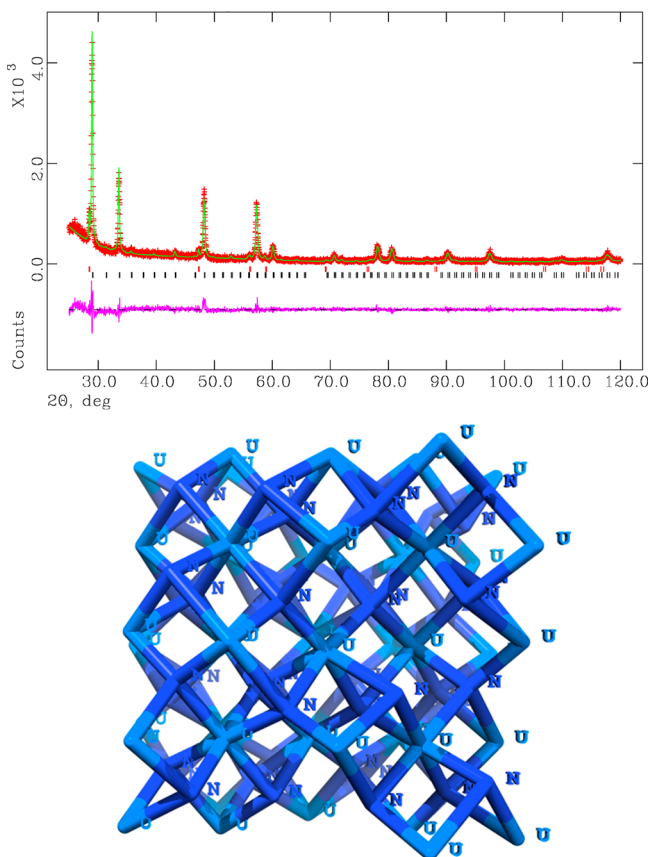


Figure 2. XRD analysis of $\text{U}_2\text{N}_{3\pm x}$ sample synthesized at 1300 °C. Experimental XRD pattern with the calculated fit (χ^2 of the fit is 2.23) are shown in the top figure (tick marks: red is for Si SRM640b internal standard, black is for the $\text{U}_2\text{N}_{3\pm x}$ phase; residue of the 2 patterns is indicated at the bottom in pink). Bottom is a model of U_2N_3 unit cell in zone [001].

at low temperatures (1100 and 1200 °C) due to incomplete reaction of reactants with the cover gas.

Figure 3 shows the XRD pattern of UN that has been synthesized by decomposing the $\text{U}_2\text{N}_{3\pm x}$ synthesized at 1300

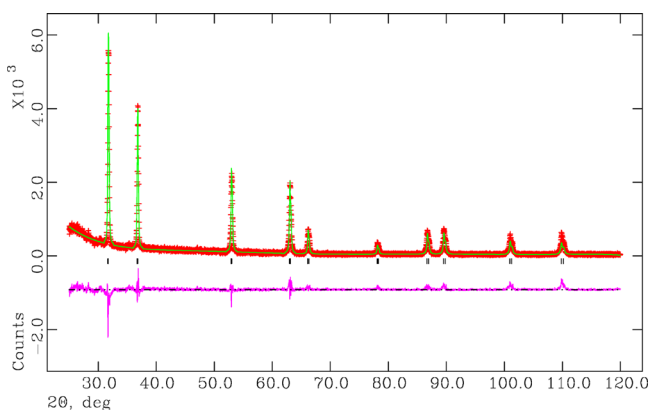


Figure 3. Powder XRD pattern of UN sample synthesized by decomposing a sample of U_2N_3 , which was synthesized at 1300 °C, in flowing Ar for 2 h (χ^2 of the fit is 2.58). Thick (red color) and thin (green color) patterns are the experimental pattern and calculated fit using the Rietveld method, respectively. Tick marks indicate the UN peak locations, while the pattern at the bottom indicates the residual between the experimental and the calculated patterns.

°C. Another powder XRD pattern of this sample was taken with Si SRM640b, and the lattice parameter of the UN product was refined to be 4.8953(1) Å. This value matches closely to a reported value of 4.8899(2) Å.⁸ The small difference (0.005 Å) in the product UN lattice parameter compared to the reported value indicates full conversion of $\text{U}_2\text{N}_{3\pm x}$ into the uranium mononitride according to reaction 2.

The $\text{U}_2\text{N}_{3\pm x}$ sample synthesized at 1300 °C contained pore spaces in its microstructure up to a considerable level (Figure 4a and 4b). The granular microstructure of $\text{U}_2\text{N}_{3\pm x}$ contains 1–

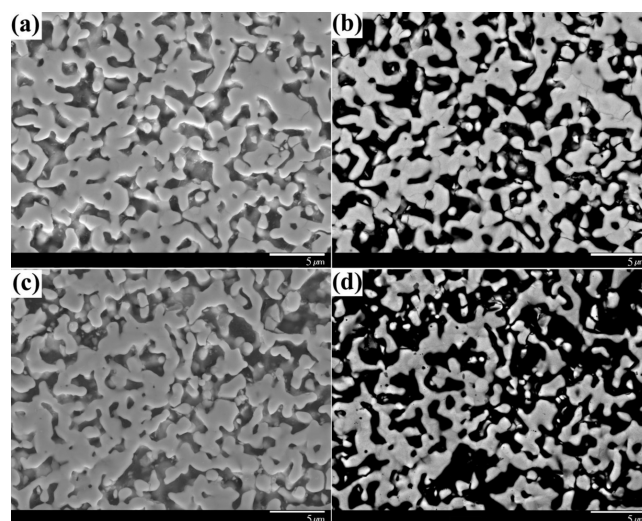


Figure 4. SEI (a and c) and BSE (b and d) SEM images of $\text{U}_2\text{N}_{3\pm x}$ (a and b) synthesized at 1300 °C and the corresponding UN (c and d) synthesized at 1100 °C.

2.5 μm wide grains. In some particle areas, these grains show stitching character that leads to an enlargement of grain size ($\sim 5 \mu\text{m}$ wide). The average length of these grains expands up to $\sim 4 \mu\text{m}$. Microstructural similarities can be observed in the as-synthesized UN sample (Figure 4c and 4d). Open pores present in UN particles indicate its potential sinterability at high temperatures.

3.3. Nitridation of $\text{UO}_2+2.15\text{C}$ Kernels at Temperatures Above 1350 °C. Five additional samples of the precursor $\text{UO}_2+2.15\text{C}$ were further nitridized at five different temperatures from 1400 to 1800 °C at 100 °C increments. Flowing N_2 gas was used as the reaction gas and as well as for cooling the samples at 1 atm. According to powder XRD, the product contained only $\text{U}_2\text{N}_{3\pm x}$ phase and no secondary mononitride or oxide phases were observed (Figure 5). Formation of sesquinitride in the cooling step under N_2 atmosphere for the samples synthesized at >1350 °C is further discussed later in the text.

Weight loss associated with nitridation of $\text{UO}_2+2.15\text{C}$ showed only a slight increase with respect to the nitridation temperature. A weight loss of $14.5 \pm 0.5\%$ was observed for all eight samples nitridized at temperatures up to 1800 °C in N_2 atmosphere followed by sample cooling in the same atmosphere, suggesting complete transformation of the reactant oxide with carbon into the sesquinitride. The absence of any reflections for graphite or C-containing chemical phases in powder XRD patterns (Figure 5) verified this suggestion. As shown in Table 1, the refined lattice parameters of these $\text{U}_2\text{N}_{3\pm x}$ showed a lattice parameter close to 10.65 Å, which reflects an approximate chemical composition of $\text{U}_2\text{N}_{3.4}$.

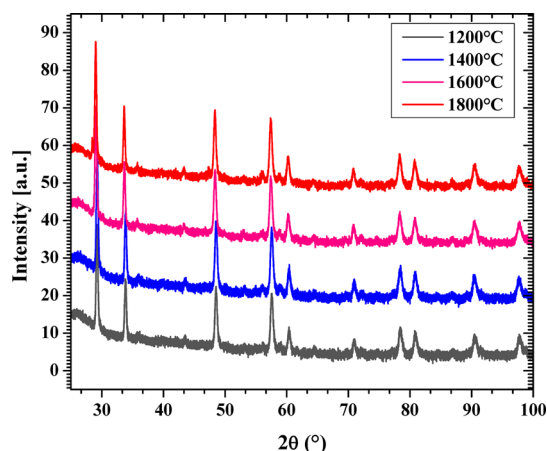


Figure 5. Experimental powder XRD patterns of $\text{U}_2\text{N}_{3\pm x}$ samples synthesized by cooling in N_2 atmosphere after nitridation of precursor oxide at 4 different temperatures. No reflections correspond to secondary UN or UO_2 phases present in the XRD patterns.

Table 1. Lattice Parameters of Uranium Nitrides as a Function of Nitridation Temperature of $\text{UO}_2+2.15\text{C}$

nitridation temp (°C)	LP (Å) of $\text{U}_2\text{N}_{3\pm x}$	χ^2 of the fit	LP (Å) of UN	χ^2 of the fit
1100	10.6461(2)	1.03	4.9069(1)	1.03
1200	10.6417(2)	1.05	4.8957(1)	2.53
1300	10.6496(2)	2.23	4.8953(1)	1.29
1400	10.6558(2)	2.22	4.8911(1)	2.2
1500	10.6488(2)	2.27	4.8927(1)	2.21
1600	10.6549(2)	2.25	4.8913(1)	2.36
1700	10.6530(2)	2.32	4.8932(1)	2.66
1800	10.6320(3)	1.48	4.8923(1)	2.54

according to literature reported lattice parameters and compositions of uranium sesquinitrides.⁹ Since uranium sesquinitride is generally designated as $\alpha\text{-U}_2\text{N}_3$ and $\beta\text{-U}_2\text{N}_3$ for N/U molar ratios of 1.54 to 1.75 and 1.45 to 1.49, respectively, the sesquinitride phase synthesized in this present work can be categorized into $\alpha\text{-U}_2\text{N}_3$.

Uranium mononitride synthesized by decomposing $\text{U}_2\text{N}_{3\pm x}$ also showed close lattice parameter values to each other (Table 1). The UN sample made using $\text{U}_2\text{N}_{3\pm x}$ synthesized at 1100 °C is an exception due to the presence of secondary UO_2 phase at a considerably high weight percentage (19 wt %). The lattice parameters of every other UN sample indicate 0.93 to 0.98 mol % of nitrogen in the UN. This reflects that the reactant $\text{U}_2\text{N}_{3\pm x}$ was virtually free of carbon, which is normally seen in the carbothermic reduction route.

Optical micrographs of a few selected $\text{U}_2\text{N}_{3\pm x}$ samples are shown in Figure 6. Other than a few minor cracks in a handful of microspheres, the kernel sphericity and integrity were well retained in the samples. The surface topology of these particles has also changed when elevated temperatures were used, probably due to severe reaction conditions and/or slight particle surface reaction with the sample crucible (Nb-1Zr alloy or Mo). The average particle size (radius) of these samples has been decreased as a function of temperature, reflecting a probable increase in the sample density (Figure 7).

Decomposition of $\text{U}_2\text{N}_{3\pm x}$ samples synthesized at different temperatures into UN also showed closely similar weight losses ($3.7 \pm 0.3\%$). These weight losses and the chemical reaction in eq 2 were utilized in determining the N/U molar ratio of

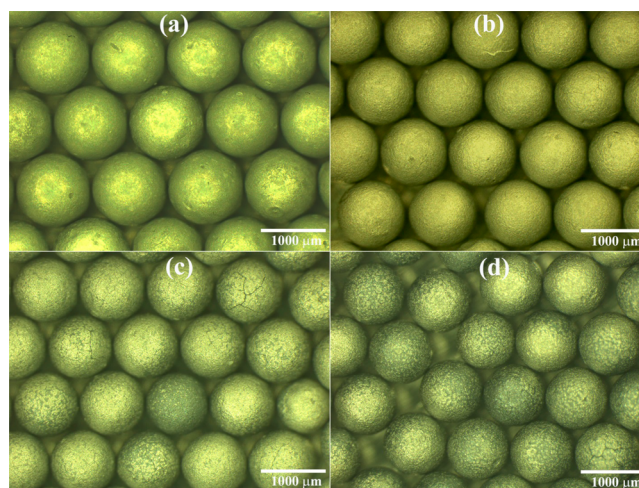


Figure 6. Optical micrographs of $\text{U}_2\text{N}_{3\pm x}$. Nitridation temperatures are (a) 1100, (b) 1300, (c) 1500, and (d) 1700 °C.

$\text{U}_2\text{N}_{3\pm x}$. The theoretical density of $\text{U}_2\text{N}_{3\pm x}$ as a function of N/U molar ratio was calculated using the formula

$$\rho = WZ/N_A V$$

where W is the molecular weight of the chemical phase, Z is the formula units, N_A is Avogadro's number, and V is the cell volume (or a^3 , where a is the lattice parameter). Figure 7 displays N/U molar ratio and geometrical densities of $\text{U}_2\text{N}_{3\pm x}$. The (geometrical) density of $\text{U}_2\text{N}_{3\pm x}$ increases slightly from 4.6 to 4.9 g/cm³ for samples synthesized at 1100 to 1200 °C (Figure 7). A considerable change in the density was observed in the samples processed to maximum temperatures of 1400 to 1600 °C, almost a linear increase in the density could be seen. Starting at a nitridation temperature of 1600 °C, $\text{U}_2\text{N}_{3\pm x}$ density reaches a plateau value of ~ 8.3 g/cm³. Overall, the $\text{U}_2\text{N}_{3\pm x}$ density increases with the increase in the nitridation temperature. The inset of Figure 7 includes theoretical densities calculated for U_2N_{3+x} (interstitial N) and U_{2-x}N_3 (vacant U) as a function of N/U molar ratio. According to these plots, the density of $\text{U}_2\text{N}_{3\pm x}$ increases as a function of N/U molar ratio if the nonstoichiometry of $\text{U}_2\text{N}_{3\pm x}$ is due to interstitial nitrogen atoms in the U_2N_3 structure rather than due to vacant uranium sites. The experimental densities also increase with an increase in the N/U molar ratio in the first four samples (from 1100 to 1400 °C) (Figure 7). The difference in the N/U ratio for these four samples ranges from 0.03 to 0.08. Therefore, it can be concluded that the defect structure of $\text{U}_2\text{N}_{3\pm x}$ in these four samples is coming from the interstitial nitrogen atoms of the unit cell. While density is still increasing, the N/U molar ratio starts to decrease in the fifth sample corresponding to 1500 °C nitridation temperature. The N/U molar ratio of the fifth sample (at 1500 °C) is 0.03 lower than that of the fourth sample (at 1400 °C). From the fifth to the eighth samples there is only a 0.005 decrease in the N/U molar ratio. The sample density also comes to a close value of 8.3 gcm⁻³, starting from the sixth sample. The decrease in the N/U molar ratio after 1400 °C sample, as supposed to an increase as shown in the U_2N_3 density vs N/U molar ratio (the inset of Figure 7), suggests some structural modifications have occurred to change the level of interstitial nitrogen atoms in the $\text{U}_2\text{N}_{3\pm x}$ unit cell in the 1400–1500 °C range.

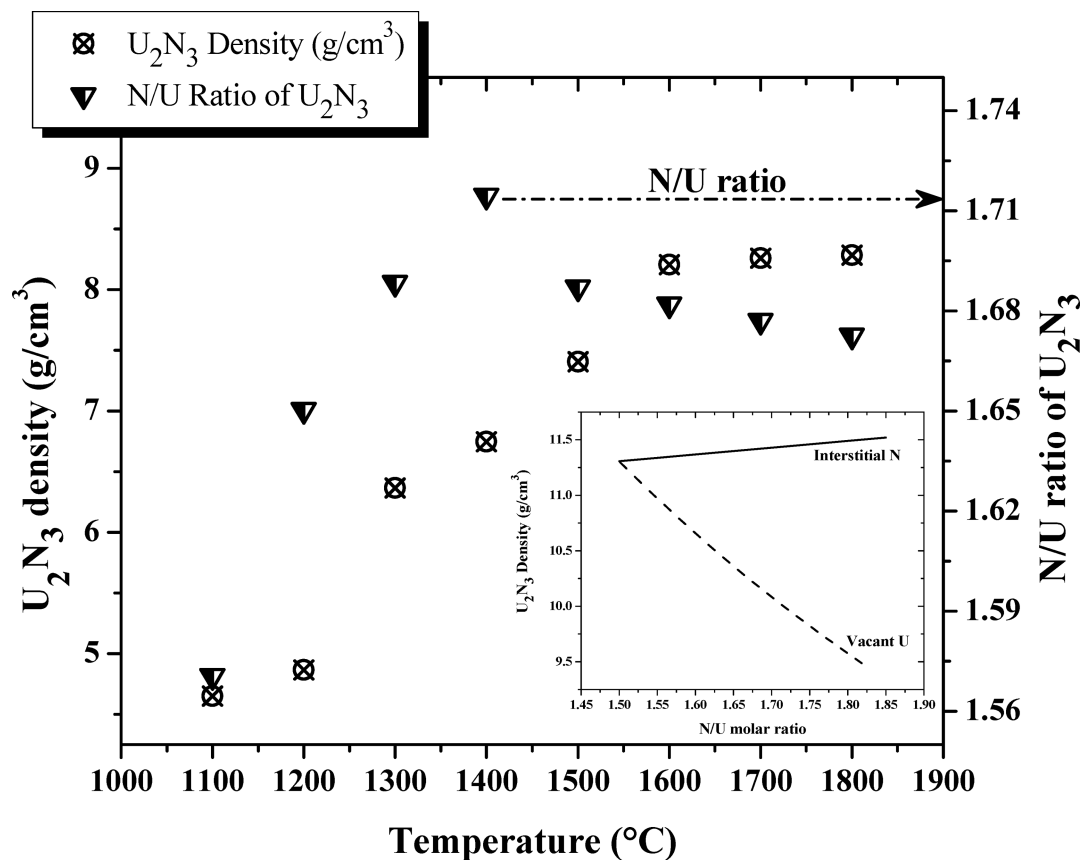
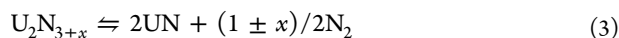


Figure 7. N/U molar ratio and geometrical density of $U_2N_{3\pm x}$ as a function of the samples' subjected temperature. (Inset) Variation of the theoretical density of $U_2N_{3\pm x}$ obtained for a nonstoichiometric unit cell, with respect to vacant U and interstitial N, as a function of N/U molar ratio.

According to U–N phase diagrams, $U_2N_{3\pm x}$ decomposes at temperatures $>1350^\circ\text{C}$ under 1 atm N_2 .^{9,10} Since low-density intermediate UN samples could react with N_2 atmosphere while the sample is being cooled, $U_2N_{3\pm x}$ can be formed at temperatures $<1350^\circ\text{C}$ according to the following equilibration¹¹



This U_2N_3 –UN– U_2N_3 equilibration might have affected the intake of nitrogen lowering the expected amount of interstitial nitrogen in the sesquinitride unit cell, resulting in a decrease in the N/U molar ratio. The density of product $U_2N_{3\pm x}$ can still increase as a function of the synthesis temperature if the low intermediate (UN) sample densities still allow the above equilibration to occur in a proper rate, so that a compact microstructure corresponding to a comparatively high density could be achieved in the product $U_2N_{3\pm x}$ during cooling. According to the present study, this occurs up to temperatures $<1600^\circ\text{C}$ (Figure 7), after which densification comes to an equilibrium value due to the difficulty of $U_2N_{3\pm x}$ formation on denser UN particle microstructure. It is also assumed that the presence of comparatively high densities observed in these samples nitridized at temperatures $\geq 1400^\circ\text{C}$, even in the presence of lower interstitial nitrogen compared to the first four samples, could be due to some effect of sintering of the samples at these elevated temperatures.

4. DISCUSSION

The generally used carbothermic reduction was modified in this study to fabricate UN kernels. In carbothermic reduction, U(C,

N) is synthesized by nitridation of carbon mixed UO_2 via an intermediate UC/ UO_2 in a single step. In this present study, $U_2N_{3\pm x}$ was made as an intermediate phase, which was thermally decomposed to pure UN. Nitridation of carbon mixed oxides ($UO_2+2.15C$) was performed in flowing nitrogen atmosphere up to a temperature of 1800°C . The cooling step was also carried out in flowing N_2 atmosphere. The resulting $U_2N_{3\pm x}$ was decomposed at 1100°C in flowing argon as the cover gas in a separate experiment. Except for the $U_2N_{3\pm x}$ sample made at 1100°C , all other samples contained a single-phase nitride (i.e., $U_2N_{3\pm x}$ or UN). Geometrical densities of $U_2N_{3\pm x}$ samples increased as a function of $UO_2+2.15C$ nitridation temperature up to 1600°C with a range of 4.6 – 8.3 g cm^{-3} . The $U_2N_{3\pm x}$ densities reached a maximum value of 8.3 g cm^{-3} for $UO_2+2.15C$ nitridation temperature of 1600°C and continued with a close density value up to 1800°C . In the case of UN, density increased almost linearly as a function of the nitridation temperature.

The phase diagrams reported for the U–N system have shown that $U_2N_{3\pm x}$ decomposes at temperatures above 1350°C forming UN, even under N_2 environments (1 atm pressure).¹² The formed UN could be transformed into $U_2N_{3\pm x}$ if N_2 was used in the sample cooling step. Thus, UN with low densities acted as an intermediate phase at temperatures above 1350°C , given the holding time at each experimented temperature was 10 h (or more for the 1100°C sample), to produce $U_2N_{3\pm x}$ when the sample was cooled in N_2 cover gas. Some other experimental work has also reported¹³ that nitrogen in the cover gas (N_2) reacts with UN to form U_2N_3 .

Ledergerber et al. indicated the feasibility of formation of the U_2N_3 phase in the sample cooling step and therefore used inert atmospheric conditions to avoid formation of such higher uranium nitride phases in UN kernel fabrication¹⁴ at temperatures ≤ 1600 °C. The observed increase in density of $U_2N_{3\pm x}$ samples and its observed constant highest value starting with the sample synthesized by nitridation of $UO_2+2.15C$ at 1600 °C and cooling in N_2 also confirms formation of stable $U_2N_{3\pm x}$ composition at lower temperatures and some effect of sintering on the samples at these high temperatures.

5. CONCLUSIONS

Microspheres of uranium mononitride (UN) by decomposing uranium sesquinitride ($U_2N_{3\pm x}$) were synthesized. Heat treatment and cooling of carbon incorporated uranium dioxide ($UO_2+2.15C$) in flowing nitrogen from 1100 to 1300 °C resulted in a single-phase uranium sesquinitride, which was confirmed by XRD studies. The sesquinitride, $U_2N_{3\pm x}$, was also identified when N_2 was used to cool the samples processed at temperatures ≥ 1400 °C. Furthermore, the as-synthesized $U_2N_{3\pm x}$ density increased from 4.7 to 8.3 g/cm³ with respect to nitridation temperature, while the UN density reached up to 9.4 g/cm³ with a lowest value of 5.8 g/cm³. Thus, formation of intact $U_2N_{3\pm x}$ was envisaged due to low-dense UN reaction with N_2 cover gas while cooling. Abrupt change in the N/U molar ratio in the samples processed at temperatures 1400–1500 °C also indicated the low intake of nitrogen atoms in the U_2N_3 unit cell corresponding to the U_2N_3 –UN– U_2N_3 transformation. Thermal decomposition of uranium sesquinitrides in inert atmosphere resulted in pure UN. Weight loss calculations indicated the sesquinitride to have a N/U molar ratio of 1.6 to 1.7, which was further confirmed using chemical compositions reported in the literature with respect to the refined lattice parameters, resulting in compositions of $U_2N_{3.2}$ to $U_2N_{3.4}$ for the sesquinitride phase fabricated in this study.

AUTHOR INFORMATION

Corresponding Author

*Phone: (865)574-6264. Fax: (865)241-3650. E-mail silvagw@ornl.gov.

Notes

The authors declare no competing financial interest.

ACKNOWLEDGMENTS

This research work was sponsored by the U.S. Department of Energy through the Office of Nuclear Energy, Science, and Technology's Fuel Cycle Research and Development Program under contract DE-AC05-00OR22725 with UT-Battelle, LLC.

REFERENCES

- (1) Hayes, S. L.; Thomas, J. K.; Peddicord, K. L. *J. Nucl. Mater.* **1990**, *171*, 262–270.
- (2) Griffiths, T. R.; Hubbard, H. V.; St, A.; Allen, G. C.; Tempest, P. A. *J. Nucl. Mater.* **1988**, *151*, 313–317.
- (3) IAEA-TECDOC-1374 report on "Development status of metallic, dispersion and non-oxide advanced and alternative fuels for power and research reactors", 2003.
- (4) Ledergerber, G.; Kopajtic, Z.; Ingold, F.; Stratton, R. W. *J. Nucl. Mater.* **1992**, *188*, 28–35.
- (5) Hunt, R. D.; Silva, C. M.; Lindemer, T. B.; Johnson, J. A.; Collins, J. L. *J. Nucl. Mater.* **2014**, *448*, 399–403.

- (6) Silva, G. W. C.; Yeaman, C. B.; Sattelberger, A. P.; Hartmann, T.; Cerefice, G. S.; Czerwinski, K. R. *Inorg. Chem.* **2009**, *48*, 10635–10642.
- (7) Larson, A. C.; Von Dreele, R. B. *Los Alamos National Laboratory Report LAUR* **2000**, 86–748.
- (8) Cordfunke, E. H. P. *J. Nucl. Mater.* **1975**, *56*, 319–326.
- (9) Tagawa, H.; Masaki, N. *J. Inorg. Nucl. Chem.* **1974**, *36*, 1099–1103.
- (10) Bugl, J.; Bauer, A. A. *J. Am. Ceram. Soc.* **1964**, *47*, 425–429.
- (11) Benz, R.; Bowman, M. G. *J. Am. Chem. Soc.* **1966**, *88*, 264–268.
- (12) Tagawa, H. *J. Nucl. Mater.* **1974**, *51*, 78–89.
- (13) Serizawa, H.; Fukuda, K.; Katsura, M. *J. Alloys Compd.* **1996**, *232*, 274–280.
- (14) Ledergerber, G.; Ingold, F.; Stratton, R. W.; Alder, H.; Prunier, C.; Warin, D.; Bauer, M. *Nucl. Technol.* **1996**, *114*, 194–204.